



Published in final edited form as:

Mol Cancer Res. 2010 November ; 8(11): 1513–1525. doi:10.1158/1541-7786.MCR-10-0262.

Mutational and Functional Analysis Reveals *ADAMTS18* Metalloproteinase as a Novel Oncogene in Melanoma

Xiaomu Wei^{1,#}, Todd D. Prickett^{1,#}, Cristina G. Vilorio², Alfredo Molinolo³, Jimmy C. Lin⁴, Isabel Cardenas-Navia¹, Pedro Cruz¹, NISC Comparative Sequencing Program¹, Steven A. Rosenberg⁵, Michael A. Davies^{6,7}, Jeffrey E. Gershenwald^{8,9}, Carlos López-Otín², and Yardena Samuels^{1,*}

¹National Human Genome Research Institute, National Institutes of Health, Bethesda, Maryland, USA

²Departamento de Bioquímica y Biología Molecular, Instituto Universitario de Oncología (IUOPA), Universidad de Oviedo, 33006-Oviedo, Spain

³Oral and Pharyngeal Cancer Branch, National Institute of Dental and Craniofacial Research, National Institutes of Health, Bethesda, Maryland, USA

⁴Ludwig Center for Cancer Genetics and Therapeutics, and Howard Hughes Medical Institute at the Johns Hopkins Kimmel Cancer Center, Baltimore, MD 21231

⁵National Cancer Institute, National Institutes of Health, Bethesda, MD 20892

⁶Department of Melanoma Medical Oncology, The University of Texas M. D. Anderson Cancer Center, Houston, Texas, 77030

⁷Department of Systems Biology, The University of Texas M. D. Anderson Cancer Center, Houston, Texas, 77030

⁸Department of Surgical Oncology, The University of Texas M. D. Anderson Cancer Center, Houston, Texas, 77030

⁹Department of Cancer Biology, The University of Texas M. D. Anderson Cancer Center, Houston, Texas, 77030

Abstract

The disintegrin-metalloproteinases with thrombospondin domains (*ADAMTS*) genes have been suggested to function as tumor suppressors as several have been found to be epigenetically silenced in various cancers. We performed a mutational analysis of the *ADAMTS* gene family in human melanoma and identified a large fraction of melanomas to harbor somatic mutations. To evaluate the functional consequences of the most commonly mutated gene, *ADAMTS18*, six of its mutations were biologically examined. *ADAMTS18* mutations had little effect on melanoma cell growth under standard conditions, but reduced cell dependence on growth factors. *ADAMTS18* mutations also reduced adhesion to laminin and increased migration *in vitro* and metastasis *in vivo*. Melanoma cells expressing mutant *ADAMTS18* had reduced cell migration after shRNA-mediated knockdown of *ADAMTS18*, suggesting that *ADAMTS18* mutations are growth-, migration- and metastasis- promoting in melanoma.

*To whom correspondence should be addressed: National Human Genome Research Institute, 50 South Drive, MSC 8000, Building 50, Room 5140, Bethesda MD 20892-8000, Phone: 301-451-2628, Fax: 301-480-9864, samuelsy@mail.nih.gov.

#These authors contributed equally to this work.

Introduction

It is widely accepted that genetics plays a major role in cancer development (1). The progression of melanoma, which is one of the most aggressive forms of skin cancer (2) is known to be accompanied by a series of genetic changes that affect at least several oncogenes and tumor suppressor genes (3). Further identification of such genes in melanoma is crucial to promote our understanding of the disease and to develop successful molecular targeted therapies. In this study, we systematically evaluated the disintegrin-metalloproteinases with thrombospondin domains (*ADAMTS*) genes through their comprehensive mutational analysis in melanoma.

The *ADAMTS* gene family is part of a superfamily of zinc-based proteinases, the metzincins (4). The matrix metalloproteinase (MMP) enzymes which also belong to the metzincins superfamily have recently been shown to be highly mutated in melanoma (5). All the *ADAMTS* proteins have proteolytic potential, but have not yet been studied in great detail in cancer (6). There is, however, an emerging concept that a number of *ADAMTS*s may have tumor suppressor activities (6–8). In particular, Vilorio *et al* have recently shown that *ADAMTS15* is somatically mutated in colorectal cancer and functional evaluation of its mutations revealed it to be a tumor suppressor gene (7). As *ADAMTS* genes encode extracellular proteins, their accessibility to systematically delivered drugs makes them excellent therapeutic targets.

In the current study, we examined melanoma samples for somatic mutations in 19 human genes that encode *ADAMTS* proteins. Remarkably, we found that one *ADAMTS* gene, *ADAMTS18*, which was highly mutated in melanoma was previously found to be a candidate cancer gene (CAN gene) in large scale whole exome sequencing of colorectal cancer (9,10). In addition to the ability of the mutated versions of this gene to cause increased proliferation of melanoma cells, we found that they increased cell migration and metastasis. These results suggest that genetic alteration of *ADAMTS18* plays a major role in melanoma tumorigenesis.

Results and Discussion

Comprehensive mutational analysis of the *ADAMTS* gene family in human melanoma

The human *ADAMTS* family consists of 19 genes (Supplementary Table 1). To evaluate whether these are genetically altered in melanoma, we analyzed the coding exons of this gene superfamily in 31 melanoma patients. A total of 408 exons from the *ADAMTS*s were extracted from genomic databases. These exons were amplified by using polymerase chain reaction (PCR) from tumor genomic DNA samples using the primers listed in Supplementary Table 2 and directly sequenced with dye terminator chemistry. We then determined whether a mutation was somatic (i.e., tumor-specific) by examining the sequence of the gene in genomic DNA from normal tissue of the relevant patient. From the ~8 Mb of sequence information obtained, we identified eleven genes containing somatic mutations (Table 1). Genes found to have one non-synonymous mutation or more were then further analyzed for mutations in an additional 48 melanomas. Through this approach, we identified 54 mutations in 11 genes, thus affecting 37% of the melanoma tumors analyzed (Table 1 and examples in Figure 1A). The number of C>T mutations in the melanoma tumors was significantly greater than other nucleotide substitutions resulting in a high prevalence of C:G>T:A transitions ($p<0.0001$) (Supplementary Figure 1), confirming previously reported melanoma signatures (11).

ADAMTS18 is highly mutated in melanoma

In order to evaluate the most highly mutated gene, *ADAMTS18* (affecting ~18% of cases analyzed), we further extended our sequencing analysis to an additional human melanoma

tumor panel consisting of 65 melanoma specimens (12). In this screen we detected 10 nonsilent somatic mutations and one silent somatic mutation, affecting approximately 14% of the cases analyzed (Supplementary Table 3 and examples in Supplementary Figure 2A), thus reaching a similar frequency of mutations observed in the first melanoma set. The mutations that arise during tumorigenesis may give a selective advantage to the tumor cell (driver mutations) or have no functional effect on tumor growth (passenger mutations). The combined genetic analysis of *ADAMTS18* in both melanoma panels identified 24 nonsynonymous and 4 synonymous mutations, yielding a ratio of nonsynonymous to synonymous changes (N/S ratio) of 6:1; this is significantly higher than the N/S ratio of 2:1 predicted for nonselected passenger mutations ($P < 0.004$) (9). These data are consistent with the hypothesis that mutations in *ADAMTS18* are positively selected for during tumorigenesis.

ADAMTS18 has been previously reported to be mutated in kidney and colorectal cancer (9,10) and (<http://www.sanger.ac.uk/genetics/CGP/Census/>). Importantly, two of the previous mutations reported in colorectal cancer lie near our reported mutations (K455T and 2085_2086insT). We therefore expanded our study to encompass 50 colorectal cancer samples. These studies revealed mutations in *ADAMTS18* in 4 of 50 colorectal cancer samples all of which were somatic (Supplementary Figure 2B). Interestingly, two of these mutations occurred exactly at the same location and cause the deletion of the same region as did the mutations in melanoma samples 98T and 85T (Table 1). A schematic representation of *ADAMTS18* protein and the location of all the mutations identified is presented in Figure 1B. The clinical information associated with the melanoma and colorectal tumors containing somatic *ADAMTS* mutations is provided in Supplementary Table 4.

***ADAMTS18* mutations promote growth factor-independent cell proliferation**

To evaluate the effect of some of these mutations on *ADAMTS* function, we decided to focus on *ADAMTS18*, which was the most highly mutated gene, harboring 14 somatic mutations in our initial screen (Table 1). The large number of mutations identified in *ADAMTS18* as well as the fact that the affected residues in *ADAMTS18* are highly conserved evolutionarily, retaining identity in rat and mouse, suggests that these mutations may be functionally important in melanoma.

To assess the effects of *ADAMT18* mutations on tumorigenic phenotypes, we created stable clones expressing wild-type or six tumor-derived *ADAMTS18* mutants (G312E, P452S, C638S, Q904X, Q1002X, P1035S) in two different human melanoma cell lines (A375 and Mel-STR (13)), both of which were confirmed to harbor wild-type *ADAMTS18*. We chose to focus on these six particular mutations as these were found in important functional domains and showed high species conservation. Western blot analysis showed a similar expression level of *ADAMT18* in A375 cells in all clones except mutations Q904X and P1035S, which had lower expression levels (Supplementary Figure 3). These clones were used for succeeding studies.

We first assessed the transformation abilities of the *ADAMTS18* mutants. As seen in Figures 2Ai–ii, expression of all the *ADAMTS18* mutants in either A375 or Mel-STR cells (except mutant Q1002X in Mel-STR cells) elicited a significantly higher cell transformation ability compared to clones expressing vector or wild-type *ADAMTS18* ($P < 0.05$, t test). When the same set of clones was evaluated for growth it was apparent that expression of wild-type or mutant *ADAMTS18* genes did not affect the growth rate of A375 and Mel-STR cells in tissue culture in the presence of media with 10% serum (Figure 2Bi–ii). However, if the serum concentration was reduced to 2.5% (for A375 cells) or 1% (for Mel-STR cells), wild-type clones grew at a slower rate than mutant clones on plastic (Fig. 2Biii–iv).

Mutant *ADAMTS18* increases cell migration through modulation of cell adhesion

ADAMTS18 is a secretory protein and similarly to virtually all *ADAMTS* family members it is strongly associated with the extracellular matrix at the pericellular space. This location likely facilitates the interaction of *ADAMTS18* with integrins and other extracellular matrix components as well as with growth factors such as VEGF and HGF (14). To test whether mutant forms of *ADAMTS18* have alterations in these interactions, we performed an adhesion assay using either fibronectin or laminin type-1 as substrates. Analysis of cell adhesion to these extracellular matrix components revealed that wild-type *ADAMTS18* expressing cells had an increased adhesion to laminin-I when compared with cells expressing the *ADAMTS18* mutations (Fig. 3Ai). In contrast, adhesion to fibronectin was similar between wild-type and mutant *ADAMTS18* expressing cells (Fig. 3Aii).

Alterations in adhesion have previously been shown to lead to changes in signaling properties. Based on the above results mutant forms of *ADAMTS18* will likely have profound effects on signaling proteins that have the ability to induce changes in gene expression programs. These effects on gene expression will ultimately result in further differences in cell adhesion and migration between *ADAMTS18*-mutant cells and wild-type cells. This situation is not unprecedented and it has been previously described in detail for other extracellular metalloproteinases including members of the *ADAMTS* family such as *ADAMTS12* (15–17).

It has previously been shown that mutations in *ADAMTS* genes can affect their cell localization (7). To test whether the identified mutations affect their localization, we immunoprecipitated concentrated conditioned media or cell lysates derived from the A375 pooled clones using FLAG-M2 beads followed by western blot analysis. Equal levels of FLAG tagged *ADAMTS18* bands were seen in immunoprecipitated cell lysates expressing WT and mutant *ADAMTS18* immunoblotted for FLAG (Figure 3Bi). However, only WT *ADAMTS18* was observed in immunoprecipitates from conditioned medium using the same clones (Figure 3Bi). Similar results were observed when the same clones were analyzed by immunofluorescent staining. As seen in Figure 3Bii, more total protein is retained and attached to the cell surface for mutant *ADAMTS18* expressing cells, explaining its absence in the conditioned medium. In contrast, immunostaining of WT *ADAMTS18* expressing cells revealed diminished cell surface localization of FLAG tagged WT protein (Figure 3Bii). The effect of *ADAMTS18* mutations on its localization could be the underlying mechanism for the differential adhesion described above.

As previous studies reported that reduced adhesion facilitates cell migration (18,19), our finding that cells expressing mutant *ADAMTS18* have reduced laminin-1 adhesion prompted us to investigate whether these cells also have increased migration ability. Boyden chamber assays showed that A375 mutant *ADAMTS18* expressing clones had an increased ability to migrate through porous membrane (Fig. 3Ci–ii) ($P < 0.05$, t test). On the basis of these results, we can postulate that *ADAMTS18* modulates cell adhesion, and this might be a candidate mechanism to explain how mutated forms of this protease stimulate cell migration.

Mutant *ADAMTS18* is required for migration in melanoma cells

To assess whether melanoma cells harboring endogenous *ADAMTS18* mutations are dependent on *ADAMTS18* for migration, we used short hairpin RNA (shRNA) to stably knock down *ADAMTS18* in melanoma lines harboring either wild-type (5T, A375) or mutant *ADAMTS18* (85T, Q1002X; 12T, P452S). We confirmed specific targeting of *ADAMTS18* by shRNAs in transfected HEK 293T cells as well as in one of the melanoma cell lines by RT-PCR (Supplementary Figures 4A and 4B). Two unique shRNA constructs

targeting *ADAMTS18* had minimal effect on the migration of cells expressing wild-type protease but substantially reduced the migration of melanoma lines carrying mutant *ADAMTS18* (Fig. 3Di–vi). Thus, mutant *ADAMTS18* is essential for the migration of melanoma cells harboring these mutations.

Mutant *ADAMTS18* causes increased metastases *in vivo*

To determine whether the *ADAMTS18* mutations affect growth *in vivo*, Mel-STR clones expressing empty vector, wild-type or mutant *ADAMTS18* were subcutaneously injected into NOD/SCID mice. Twenty two days after injection, the mice were evaluated for skin ulceration as well as metastasis formation by examining hematoxylin/eosin (H&E) stained sections of paraffin embedded lungs. As seen in Figure 4A, most of the tumors expressing mutant *ADAMTS18* presented with ulcerations whereas few of the mice with cells expressing wild-type *ADAMTS18* had ulcerating lesions. In addition, most mice injected with mutant *ADAMTS18* expressing cells had micrometastases. In contrast, no lung metastases were found in the mice injected with wild-type clones (Figures 4B and 4C). This suggests that, in some cases, *ADAMTS18* may have an assay-specific suppressive effect. This scenario has precedent and has been described for *Mdm2* (20). Although the underlying mechanism for the lack of a metastatic phenotype seen in the wild-type cells is unclear, it is consistent with *ADAMTS* proteins being inhibited by proteins such as TIMPs (Tissue Inhibitor of Metalloproteinases) *in vivo* (21). It must be noted, though, that the number of identified endogenous protease inhibitors is significantly lower than that of proteases (22). It is therefore conceivable that another, as yet unknown, *ADAMTS18* inhibitor is being expressed *in vivo*, specifically inhibiting the metastasis of cells expressing wild-type *ADAMTS18*.

Clearly, *ADAMTS18* mutations are dispersed throughout its domains. This is reminiscent to the driver mutations reported in *ERBB4* (23), *CARD11* (24) and *FLT3* (25). In addition to the catalytic domain, *ADAMTS* proteins have non-catalytic ancillary domains that regulate interaction of the protein with substrates or inhibitors such as the TIMPs, and these domains have been shown to mediate recognition and cleavage of numerous substrates (26–28). Furthermore, the ancillary domain of several *ADAMTS* proteins is modified by C-terminal proteolysis (29–31), which might alter substrate recognition and enzyme localization. As several of the mutations identified in *ADAMTS18* lie within the C-terminus and some cause its truncation, they might affect this recognition. Thus elucidation of the specific interactions of *ADAMTS18* with particular substrate(s) will provide an important understanding of the biochemical effects of the discovered mutations. Recently, a novel method of detecting protease substrates has been developed by Kleifeld *et al* (32). Upon radioisotopic labeling of the N-termini amine groups of cellular proteins and enzymatic reaction with known proteases, fragmented peptides are purified and run on a MS/MS thus identifying new cleavage sites. Utilization of such a detection method in determining the physiological substrates for *ADAMTS18* will prove beneficial.

As mentioned above, several *ADAMTS*s have been suggested to harbor antitumorigenic properties (33,34). These reports focused on the anti-angiogenic effects of *ADAMTS1* and *ADAMTS8* (35,36) as well as the modulation of the extracellular signal-regulated kinase (ERK) pathway by *ADAMTS12* through extracellular matrix (ECM) interactions (15). El Hour *et al* demonstrated that lack of *ADAMTS12* in mice resulted in increased angiogenesis and tumor progression (37). In addition, *ADAMTS15* was shown to have a protective role in breast cancer as increased expression along with decreased expression of *ADAMTS8* resulted in prolonged relapse-free progression in these patients (38). Genetic inactivation of *ADAMTS15* via somatic mutation lead to decreased ability to suppress colony-formation or invasion of colorectal cancer cells compared with expression of the wild-type gene (7). Furthermore, epigenetic silencing of *ADAMTS* genes such as *ADAMTS9* or *ADAMTS18*

has been observed in different types of carcinomas implying them to be tumor suppressors (39,40)

Conversely, genetic silencing of ADAMTS20 in mice resulted in increased melanoblast apoptosis, decreased soluble Kit ligand (sKitl) stimulation of the pro-survival pathway, and decreased processing of the ECM protein versican (41). These results suggest that ADAMTS20 is a pro-survival molecule that might act as an oncogene in melanoma. This is supported by the observation that ADAMTS20 is overexpressed in brain, colon and breast cancers (42). Importantly, ADAMTS20 was the second most highly mutated gene in our study harboring 12 somatic mutations (11.4%). Future functional evaluation of the identified mutations in ADAMTS20 will further verify whether ADAMTS20 participates in melanoma progression.

Taken together, our results provide genetic, cellular and *in vivo* evidence that ADAMTS18 has a role in promoting melanoma tumorigenesis. We postulate that the genetic alteration of ADAMTS18 contributes to the aggressive biological behavior of melanoma through modulation of proliferative, migratory and metastatic mechanisms. Importantly, this is the first genetic identification of an ADAMTS gene that is functionally proven to have an oncogenic role in human disease.

Materials and Methods

Tumor Tissues

Tissue and melanoma cell lines used for the discovery and first validation in this study were described previously (5).

For the melanoma second validation set, Optimum cutting temperature (OCT)-embedded frozen clinical specimens were obtained from the Melanoma Informatics, Tissue Resource, and Pathology Core, and the Central Nervous System Tissue Bank at The University of Texas M. D. Anderson Cancer Center under Institutional Review Board-approved protocols. H&E-guided dissection and isolation of DNA from the tumor-enriched isolates has been described previously (12).

PCR, sequencing and mutational analysis of melanoma samples

PCR and sequencing was done as previously described (5,7,23). The primary phase mutation screen was analyzed using Consed (43). Variants were called using Polyphred 6.11 (44) and DIPDetector, an indel detector for improved sensitivity in finding insertions and deletions. Sequence traces of the secondary screen were analyzed using the Mutation Surveyor software package (SoftGenetics, State College, PA).

To increase our confidence that the mutations in the M. D. Anderson set, for which no matched normal DNA sample was available, did not represent germline polymorphisms, we searched the corresponding exons of *ADAMTS18* in a total of 145 DNA samples and detected no abnormalities.

Construction of wild-type and mutant *ADAMTS18* expression vector

Human *ADAMTS18* (NM_199355.2) was cloned by PCR as previously described(5) using a clone (#30343625) purchased from Open Biosystems with primers in Supplementary Table S5. The PCR product was cloned into the mammalian expression vector pCDF-MCS2-EF1-Puro™ (Systems Biosciences, Inc., Mountain View, CA) or pCDNA3.1 (-) (Invitrogen) via the XbaI and NotI restriction sites. The G312E, P452S, C638S, Q904X, Q1002X, and

P1035S point mutants were made using Phusion PCR for site-directed mutagenesis using the primers listed in Supplementary Table S5.

Cell culture and transient expression

Metastatic melanoma tumor lines were maintained as previously described (45). HEK 293T cells were purchased from ATCC (Manassas, VA) and maintained in complete Dulbecco's Modified Eagles Medium (DMEM) supplemented with 10% Fetal Bovine Serum (FBS), 1× non-essential amino acids, 2 mM L-glutamine, and 0.75% sodium bicarbonate. A375 cells were purchased from National Cancer Institute, Division of Cancer Treatment, Developmental Therapeutics Program, Frederick, MD and maintained in RPMI-1640 and supplemented with 10% FBS. Mel-STR cells were described previously(5). HEK 293T cells were transfected with Lipofectamine2000 reagent (Invitrogen, Carlsbad, CA) at a 6:1 ratio with DNA (μl:μg) using 3–5 μg of plasmid DNA per T75 flask.

Immunoprecipitation and western blotting

Transfected cells were gently washed 3× in PBS and then lysed using 0.5–1.0 mL 1% NP-40 lysis buffer (1% NP-40, 50mM Tris-HCl pH 7.5, 150mM NaCl, Complete Protease Inhibitor tablet, EDTA-free (Roche, Indianapolis, IN), 1μM sodium orthovanadate, 1 mM sodium fluoride, and 0.1% β-mercaptoethanol) per T-75 flask, for 20 min on ice. Lysed cells were scraped and transferred into a 1.5 mL microcentrifuge tube. Extracts were centrifuged for 10 min at 14,000 rpm at 4°C. 500 μl of supernatant was immunoprecipitated overnight using 20 μL of anti-FLAG (M2) beads (Sigma-Aldrich A2220). Immunoprecipitation of conditioned medium was done as previously described (5). The immunoprecipitates were washed and subjected to SDS-PAGE and western blotting as previously described (46). Primary antibodies used in our analysis were anti-FLAG horseradish peroxidase conjugated (Sigma-Aldrich A8592) and anti-alpha-tubulin (Calbiochem-EMD Biosciences, Gibbstown, NJ CP06).

Pooled stable expression

To make lentivirus, pCDF-MCS2-EF1-Puro *ADAMTS18* constructs were co-transfected into HEK 293T cells seeded at 1.5×10^6 per T75 flask with pVSV-G and pFIV-34N (kind gifts from Todd Waldman, Georgetown University) helper plasmids using Lipofectamine 2000 as described by the manufacturer. Virus-containing media was harvested 48–60hr after transfection, filtered, aliquoted and stored at -80°C .

A375 cells were seeded at 1.5×10^6 cells per T75 flask 24 hr prior to infection. Lentivirus for *ADAMTS18* (WT, G312E, P452S, C638S, Q904X, Q1002X, and P1035S) or empty vector control were used to infect A375 cells as previously described(47). Stable expression of *ADAMTS18* proteins (WT and mutants) was determined by SDS-PAGE analysis followed by immunoprecipitation and immunoblotting with anti-FLAG and anti-alpha-tubulin to show equivalent expression among pooled clones.

Mel-STR cells were seeded at 1.5×10^6 per T75 flask 24 hr prior to transfection with *ADAMTS18* (WT, G312E, P452S, C638S, Q904X, Q1002X, and P1035S) or empty vector control in pcDNA3.1(-) using Fugene6 (Roche 11814443001) as per manufacturers protocol. Transfected cells were selected using normal complete growth medium supplemented with 300μg/ml G418 and pooled for future experiments. Stable expression of *ADAMTS18* proteins (WT and mutants) was determined by SDS-PAGE analysis followed by immunoprecipitation and immunoblotting with anti-FLAG and anti-alpha-tubulin to show equivalent expression among pools.

Lentiviral shRNA

Constructs for stable depletion of ADAMTS18 were obtained from Open Biosystems (Huntsville, AL) and two were confirmed to efficiently knockdown ADAMTS18 at the message and protein level. Lentiviral stocks were prepared as previously described (5). Melanoma cell lines (5T, 12T, 85T and A375) were infected with shRNA lentiviruses for each condition (vector and scrambled controls and three independent *ADAMTS18*-specific shRNAs whose sequences are presented in Supplementary table S6). Selection and growth were done as described above. Stably infected pooled clones were tested in functional assays.

Reverse Transcription PCR

Total RNA was extracted from pooled clones of melanoma cells A375 stably knocked-down for endogenous ADAMTS18 following the manufacturer's protocol for RNeasy Mini Kit (Qiagen #74101). Total RNA was eluted in 30 μ l DEPC-treated dH₂O. A total of 1 μ g of total RNA was used for single strand cDNA synthesis using a SuperScript III First Strand kit (Invitrogen #18080-051). cDNA was amplified using the oIdo dT20 primer supplied in the kit. To test for loss of ADAMTS18 message we used 1 μ l of cDNA in the PCR with either ADAMTS18 primers (forward primer: 5'-acctggctcagtggtcca-3' and reverse primer: 5'-tgcaggtctctccaagtc-3'), (forward primer: 5'-ccgtttgtggttgagtatg-3' and reverse primer: 5'-cgctagaacctggacagaa-3') or GAPDH primers (forward primer: 5'-tggaaggactcatgaccaca-3' and reverse primer: 5'-tgctgtagccaaattcgtt-3'). The product was then analyzed on a 1% agarose gel.

Proliferation assays

To examine growth potential, pooled A375 and Mel-STR ADAMTS18 clones were seeded into 96 well plates at 250 cells per well in either 1%, 2.5% or 10% serum-containing medium and incubated for 13–17 days. Cell numbers were counted every 48 hr by lysing cells in 50 μ l 0.2% SDS/well and incubating for 2 hours at 37°C prior to addition of 150 μ l/well of SYBR Green I solution (1:750 SYBR Green I (Invitrogen-Molecular Probes) diluted in dH₂O). Plates were analyzed using a BMG Labtech FLOUstar Optima.

Foci formation assays

A375 and Mel-STR pooled clones were seeded at 500 cells per T25 flask in normal complete serum containing medium and incubated for 8–10 days prior to staining with Hema 3 Stat Pack (Protocol) to visualize foci for counting.

Migration assays

A375 or melanoma cells with stable knock-down of ADAMTS18 were seeded into pre-conditioned migration wells (8.0 μ m – BD Biocoat, BD Biosciences) at 10,000 to 30,000 cells per well in serum-free medium in the top chamber and incubated for 16–18 hr with complete serum containing medium in the bottom chamber prior to harvesting. Inserts were fixed and stained using Hema 3 Stat Pack (Protocol). Inserts were analyzed and counted for cells migrated per field view and quantitated using ImageJ (NIH software).

Adhesion assay

96-well plates were coated with 5 μ g/ml laminin-I or 5 μ g/ml fibronectin in 200 μ l 1 \times PBS and incubated overnight at 4°C. Prior to plating cells the coated wells were washed once in PBS and then blocked with 0.1mg/ml heat-inactivated BSA (dissolved in PBS) for 1 hr at room temperature. Cells were seeded into the plates at 30,000 cells per well and incubated at 37°C for 2 hr with the lid off. Cells were shaken off plate vigorously then washed three times with PBS. Remaining cells were fixed using 4% paraformaldehyde in PBS overnight

at 4°C. Plates were then washed three times using ddH₂O. Attached cells were stained with 0.1% crystal violet (w/v – 20% methanol in PBS) for 30 min at room temperature followed by three washes with dd H₂O. Dye was solubilized with 0.1N HCl for 10 min at room temperature. Absorbance was measured at 610nm on Molecular Devices SpectraMax and quantitated using Microsoft Excel.

Immunofluorescent analysis of pooled clones

A375 pooled ADAMTS18 clones expressing either (WT, G312E, C638S and P1035S) or empty vector were seeded on 8-well chamber slides at a cell density of 50,000 cells per well. Cells were grown for 24 hr prior to fixing and staining. Chamber slides were washed once with 1× PBS followed by fixation with 4% paraformaldehyde (PBS) for 15 min at room temperature. Cells were subsequently washed three times with ice-cold 1× PBS for 5 min per wash. Slides were blocked with 1% BSA (PBS-T) for 30–60 min at room temperature followed by washing with 1× PBS twice. Chamber slides were immunostained with anti-FLAG (rabbit) (Sigma-cat# F7425) in 1% BSA (PBS-T) at a dilution of 1:50 for 18 hr at 4°C. Chamber slides were washed three times with PBS at 5 min per wash followed by incubation with anti-rabbit (Alexa fluor 568-cat# A11036) (Invitrogen, Carlsbad, CA) diluted at 1:200 in 1% BSA (PBS-T) for 2 hr at room temperature. Slides were washed three times in PBS followed by fixation/mounting with DAPI and analyzed on a Zeiss A×10 (Scope.A1) at 40× using SPOT imaging software for image acquisition. Further analysis was done using Adobe Photoshop and ImageJ/NIH software.

Xenograft Studies in Mice

NOD/SCID mice were purchased from Jackson Laboratories. All mice were housed in a pathogen-free facility and were given autoclaved food and water. Mel-STR pooled clones expressing empty vector or with wild-type *ADAMTS18* or mutant *ADAMTS18* were grown up in T-75 flasks to 70–80% confluency. 1×10^6 cells were resuspended in 100 μ L of sterile 1×PBS and injected subcutaneously into 11 week old male NOD/SCID mice. Mice were monitored bi-weekly and final tumor weights were measured after tumor was excised from euthanized mice at day 22 post-injection. Lungs from each mouse were harvested in 4% paraformaldehyde and embedded in paraffin for H&E staining followed by histological evaluation.

Statistical analysis

Statistical analyses were performed using the R statistical environment and Microsoft Excel (two-tailed t-test, binomial test).

Supplementary Material

Refer to Web version on PubMed Central for supplementary material.

Acknowledgments

We thank for technical assistance Allison Burrell, Catherine Y. Cheng and Dr. Kristin E. Yates. We thank Dr. Robert Weinberg for the Mel-STR cell line and Dr. Gabriel Capellá for colorectal cancer samples. We also thank Drs Lynn Matrisian, Suneel Apte, Daniel McCulloch and Paul Meltzer, for their helpful comments. We also thank members of the NISC Comparative Sequencing Program for providing leadership in the generation of the sequence data analyzed here. Funded by the National Human Genome Research Institute, National Institutes of Health to Y.S. and Ministerio de Ciencia e Innovación-Spain, Fundación “M. Botín”, and European Union (FP7 MicroEnviMet) to C.L.-O. Supported in part by the University of Texas M. D. Anderson Cancer Center Melanoma Specialized Programs of Research Excellence (SPORE) and the Melanoma Informatics, Tissue Resource, and Pathology Core (grant P50 CA93459).

References

1. Vogelstein B, Kinzler KW. Cancer genes and the pathways they control. *Nat Med.* 2004; 10:789–799. [PubMed: 15286780]
2. Jemal A, Siegel R, Ward E, Hao Y, Xu J, Thun MJ. Cancer statistics, 2009. *CA: a cancer journal for clinicians.* 2009; 59:225–249. [PubMed: 19474385]
3. Curtin JA, Fridlyand J, Kageshita T, Patel HN, Busam KJ, Kutzner H, et al. Distinct sets of genetic alterations in melanoma. *The New England journal of medicine.* 2005; 353:2135–2147. [PubMed: 16291983]
4. Stocker W, Bode W. Structural features of a superfamily of zinc-endopeptidases: the metzincins. *Curr Opin Struct Biol.* 1995; 5:383–390. [PubMed: 7583637]
5. Palavalli LH, Prickett TD, Wunderlich JR, Wei X, Burrell AS, Porter-Gill P, et al. Analysis of the matrix metalloproteinase family reveals that MMP8 is often mutated in melanoma. *Nature genetics.* 2009; 41:518–520. [PubMed: 19330028]
6. Rocks N, Paulissen G, El Hour M, Quesada F, Crahay C, Gueders M, et al. Emerging roles of ADAM and ADAMTS metalloproteinases in cancer. *Biochimie.* 2008; 90:369–379. [PubMed: 17920749]
7. Vilorio CG, Obaya AJ, Moncada-Pazos A, Llamazares M, Astudillo A, Capella G, et al. Genetic inactivation of ADAMTS15 metalloprotease in human colorectal cancer. *Cancer research.* 2009; 69:4926–4934. [PubMed: 19458070]
8. Li Z, Zhang W, Shao Y, Zhang C, Wu Q, Yang H, et al. High-resolution melting analysis of ADAMTS18 methylation levels in gastric, colorectal and pancreatic cancers. *Medical oncology (Northwood, London, England).* 2009
9. Sjoblom T, Jones S, Wood LD, Parsons DW, Lin J, Barber TD, et al. The consensus coding sequences of human breast and colorectal cancers. *Science (New York, NY).* 2006; 314:268–274.
10. Wood LD, Parsons DW, Jones S, Lin J, Sjoblom T, Leary RJ, et al. The Genomic Landscapes of Human Breast and Colorectal Cancers. *Science (New York, NY).* 2007
11. Greenman C, Stephens P, Smith R, Dalgliesh GL, Hunter C, Bignell G, et al. Patterns of somatic mutation in human cancer genomes. *Nature.* 2007; 446:153–158. [PubMed: 17344846]
12. Davies MA, Stemke-Hale K, Lin E, Tellez C, Deng W, Gopal YN, et al. Integrated Molecular and Clinical Analysis of AKT Activation in Metastatic Melanoma. *Clin Cancer Res.* 2009; 15:7538–7546. [PubMed: 19996208]
13. Gupta PB, Kuperwasser C, Brunet JP, Ramaswamy S, Kuo WL, Gray JW, et al. The melanocyte differentiation program predisposes to metastasis after neoplastic transformation. *Nature genetics.* 2005; 37:1047–1054. [PubMed: 16142232]
14. Mochizuki S, Okada Y. ADAMs in cancer cell proliferation and progression. *Cancer science.* 2007; 98:621–628. [PubMed: 17355265]
15. Llamazares M, Obaya AJ, Moncada-Pazos A, Heljasvaara R, Espada J, Lopez-Otin C, et al. The ADAMTS12 metalloproteinase exhibits anti-tumorigenic properties through modulation of the Ras-dependent ERK signalling pathway. *Journal of cell science.* 2007; 120:3544–3552. [PubMed: 17895370]
16. Gutierrez-Fernandez A, Fueyo A, Folgueras AR, Garabaya C, Pennington CJ, Pilgrim S, et al. Matrix metalloproteinase-8 functions as a metastasis suppressor through modulation of tumor cell adhesion and invasion. *Cancer research.* 2008; 68:2755–2763. [PubMed: 18413742]
17. Lopez-Otin C, Hunter T. The regulatory crosstalk between kinases and proteases in cancer. *Nat Rev Cancer.* 2010; 10:278–292. [PubMed: 20300104]
18. Yamagata M, Suzuki S, Akiyama SK, Yamada KM, Kimata K. Regulation of cell-substrate adhesion by proteoglycans immobilized on extracellular substrates. *The Journal of biological chemistry.* 1989; 264:8012–8018. [PubMed: 2470739]
19. Touab M, Villena J, Barranco C, Arumi-Uria M, Bassols A. Versican is differentially expressed in human melanoma and may play a role in tumor development. *The American journal of pathology.* 2002; 160:549–557. [PubMed: 11839575]
20. Manfredi JJ. The Mdm2-p53 relationship evolves: Mdm2 swings both ways as an oncogene and a tumor suppressor. *Genes & development.* 2010; 24:1580–1589. [PubMed: 20679392]

21. Yu WH, Yu S, Meng Q, Brew K, Woessner JF Jr. TIMP-3 binds to sulfated glycosaminoglycans of the extracellular matrix. *The Journal of biological chemistry*. 2000; 275:31226–31232. [PubMed: 10900194]
22. Lopez-Otin C, Bond JS. Proteases: multifunctional enzymes in life and disease. *The Journal of biological chemistry*. 2008; 283:30433–30437. [PubMed: 18650443]
23. Prickett TD, Agrawal NS, Wei X, Yates KE, Lin JC, Wunderlich JR, et al. Analysis of the tyrosine kinome in melanoma reveals recurrent mutations in ERBB4. *Nature genetics*. 2009; 41:1127–1132. [PubMed: 19718025]
24. Lenz G, Davis RE, Ngo VN, Lam L, George TC, Wright GW, et al. Oncogenic CARD11 mutations in human diffuse large B cell lymphoma. *Science (New York, NY)*. 2008; 319:1676–1679.
25. Meshinchi S, Appelbaum FR. Structural and functional alterations of FLT3 in acute myeloid leukemia. *Clin Cancer Res*. 2009; 15:4263–4269. [PubMed: 19549778]
26. Kashiwagi M, Enghild JJ, Gendron C, Hughes C, Caterson B, Itoh Y, et al. Altered proteolytic activities of ADAMTS-4 expressed by C-terminal processing. *The Journal of biological chemistry*. 2004; 279:10109–10119. [PubMed: 14662755]
27. Gendron C, Kashiwagi M, Lim NH, Enghild JJ, Thogersen IB, Hughes C, et al. Proteolytic activities of human ADAMTS-5: comparative studies with ADAMTS-4. *The Journal of biological chemistry*. 2007; 282:18294–18306. [PubMed: 17430884]
28. Fushimi K, Troeberg L, Nakamura H, Lim NH, Nagase H. Functional differences of the catalytic and non-catalytic domains in human ADAMTS-4 and ADAMTS-5 in aggrecanolytic activity. *The Journal of biological chemistry*. 2008; 283:6706–6716. [PubMed: 18156631]
29. Rodriguez-Manzaneque JC, Milchanowski AB, Dufour EK, Leduc R, Iruela-Arispe ML. Characterization of METH-1/ADAMTS1 processing reveals two distinct active forms. *The Journal of biological chemistry*. 2000; 275:33471–33479. [PubMed: 10944521]
30. Somerville RP, Jungers KA, Apte SS. Discovery and characterization of a novel, widely expressed metalloprotease, ADAMTS10, and its proteolytic activation. *The Journal of biological chemistry*. 2004; 279:51208–51217. [PubMed: 15355968]
31. Flannery CR, Zeng W, Corcoran C, Collins-Racie LA, Chockalingam PS, Hebert T, et al. Autocatalytic cleavage of ADAMTS-4 (Aggrecanase-1) reveals multiple glycosaminoglycan-binding sites. *The Journal of biological chemistry*. 2002; 277:42775–42780. [PubMed: 12202483]
32. Kleifeld O, Doucet A, auf dem Keller U, Prudova A, Schilling O, Kainthan RK, et al. Isotopic labeling of terminal amines in complex samples identifies protein N-termini and protease cleavage products. *Nature biotechnology*. 28:281–288.
33. Balbin M, Fueyo A, Tester AM, Pendas AM, Pitiot AS, Astudillo A, et al. Loss of collagenase-2 confers increased skin tumor susceptibility to male mice. *Nature genetics*. 2003; 35:252–257. [PubMed: 14517555]
34. Lopez-Otin C, Matrisian LM. Emerging roles of proteases in tumour suppression. *Nat Rev Cancer*. 2007; 7:800–808. [PubMed: 17851543]
35. Vazquez F, Hastings G, Ortega MA, Lane TF, Oikemus S, Lombardo M, et al. METH-1, a human ortholog of ADAMTS-1, and METH-2 are members of a new family of proteins with angiogenic-inhibitory activity. *The Journal of biological chemistry*. 1999; 274:23349–23357. [PubMed: 10438512]
36. Dunn JR, Reed JE, du Plessis DG, Shaw EJ, Reeves P, Gee AL, et al. Expression of ADAMTS-8, a secreted protease with antiangiogenic properties, is downregulated in brain tumours. *British journal of cancer*. 2006; 94:1186–1193. [PubMed: 16570050]
37. El Hour M, Moncada-Pazos A, Blacher S, Masset A, Cal S, Berndt S, et al. Higher sensitivity of Adamts12-deficient mice to tumor growth and angiogenesis. *Oncogene*. 2010; 29:3025–3032. [PubMed: 20208563]
38. Porter S, Clark IM, Kevorkian L, Edwards DR. The ADAMTS metalloproteinases. *The Biochemical journal*. 2005; 386:15–27. [PubMed: 15554875]
39. Lo PH, Leung AC, Kwok CY, Cheung WS, Ko JM, Yang LC, et al. Identification of a tumor suppressive critical region mapping to 3p14.2 in esophageal squamous cell carcinoma and studies

- of a candidate tumor suppressor gene, ADAMTS9. *Oncogene*. 2007; 26:148–157. [PubMed: 16799631]
40. Jin H, Wang X, Ying J, Wong AH, Li H, Lee KY, et al. Epigenetic identification of ADAMTS18 as a novel 16q23.1 tumor suppressor frequently silenced in esophageal, nasopharyngeal and multiple other carcinomas. *Oncogene*. 2007; 26:7490–7498. [PubMed: 17546048]
 41. Silver DL, Hou L, Somerville R, Young ME, Apte SS, Pavan WJ. The secreted metalloprotease ADAMTS20 is required for melanoblast survival. *PLoS Genet*. 2008; 4:e1000003. [PubMed: 18454205]
 42. Llamazares M, Cal S, Quesada V, Lopez-Otin C. Identification and characterization of ADAMTS-20 defines a novel subfamily of metalloproteinases-disintegrins with multiple thrombospondin-1 repeats and a unique GON domain. *The Journal of biological chemistry*. 2003; 278:13382–13389. [PubMed: 12562771]
 43. Gordon D, Abajian C, Green P. Consed: a graphical tool for sequence finishing. *Genome research*. 1998; 8:195–202. [PubMed: 9521923]
 44. Bhangale TR, Stephens M, Nickerson DA. Automating resequencing-based detection of insertion-deletion polymorphisms. *Nature genetics*. 2006; 38:1457–1462. [PubMed: 17115056]
 45. Chappell DB, Zaks TZ, Rosenberg SA, Restifo NP. Human melanoma cells do not express Fas (Apo-1/CD95) ligand. *Cancer research*. 1999; 59:59–62. [PubMed: 9892185]
 46. Samuels Y, Wang Z, Bardelli A, Silliman N, Ptak J, Szabo S, et al. High frequency of mutations of the PIK3CA gene in human cancers. *Science (New York, NY)*. 2004; 304:554.
 47. Solomon DA, Kim JS, Cronin JC, Sibenaller Z, Ryken T, Rosenberg SA, et al. Mutational inactivation of PTPRD in glioblastoma multiforme and malignant melanoma. *Cancer research*. 2008; 68:10300–10306. [PubMed: 19074898]

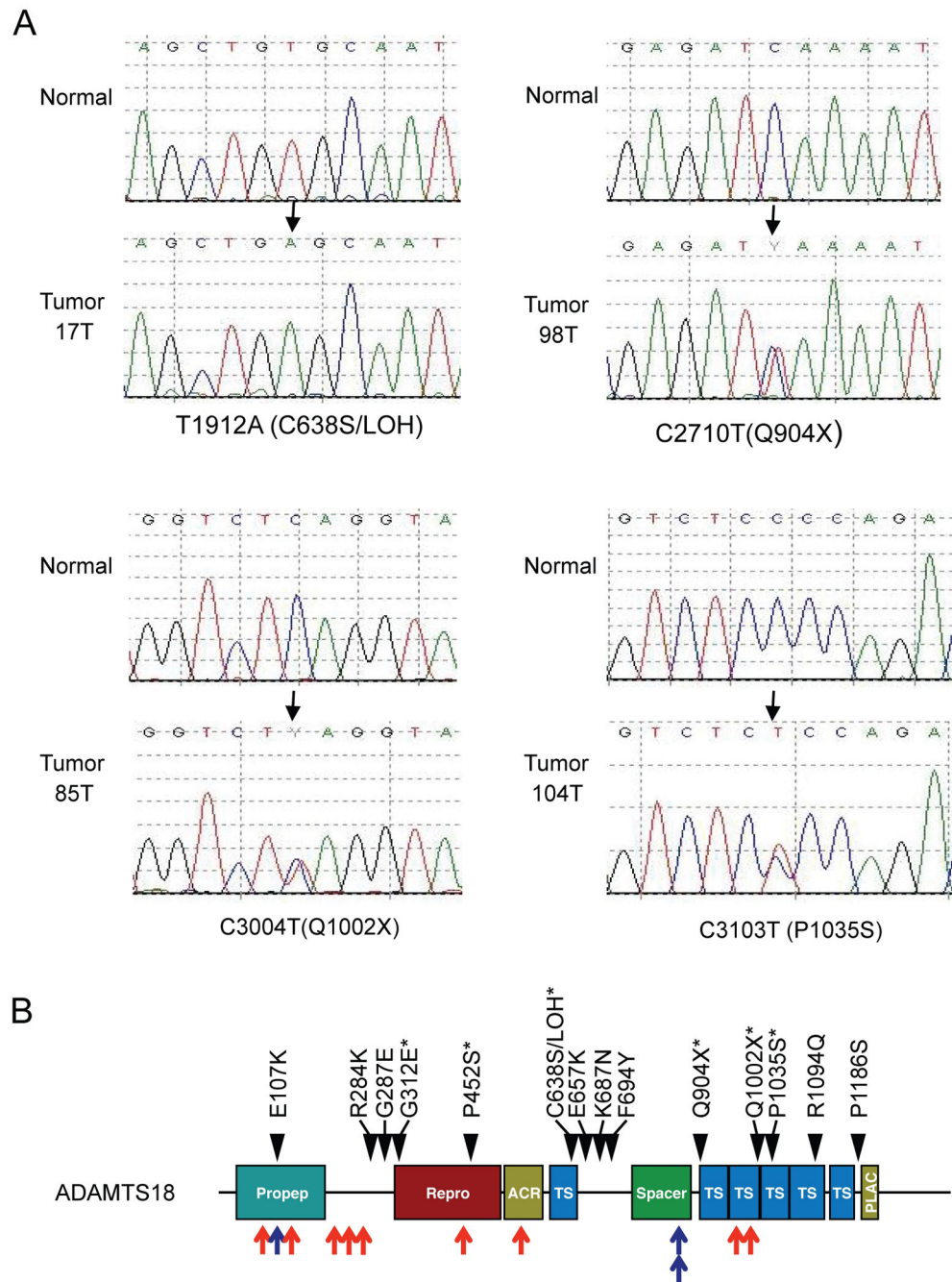


Figure 1. Somatic mutations identified in *ADAMTS18* in different cancer types

(A) Representative sequence chromatograms of mutations identified in *ADAMTS18*. In each case, the lower sequence chromatogram was from melanoma tumor. The top sequence chromatograms were from normal tissue of the relevant patient. Arrows indicate the location of missense mutations. The nucleotide and amino acid alterations are shown at the bottom of each chromatogram. (B) Protein schematic of *ADAMTS18* is presented with conserved functional domains indicated as colored blocks. Black arrow heads indicate positions of nonsynonymous somatic mutations identified in 79 melanoma specimens. Mutations found in the validation melanoma or colorectal specimens are labeled as red or blue arrows, respectively. The mutations analyzed in this study are indicated with an asterisk. Propep:

Reprolysin family propeptide domain; Repro: Reprolysin family zinc metalloprotease domain; ACR: ADAM cysteine-rich domain; TS: Thrombospondin type 1 domain; Spacer: ADAMTS Spacer 1 domain; PLAC: Protease and lacunin domain.

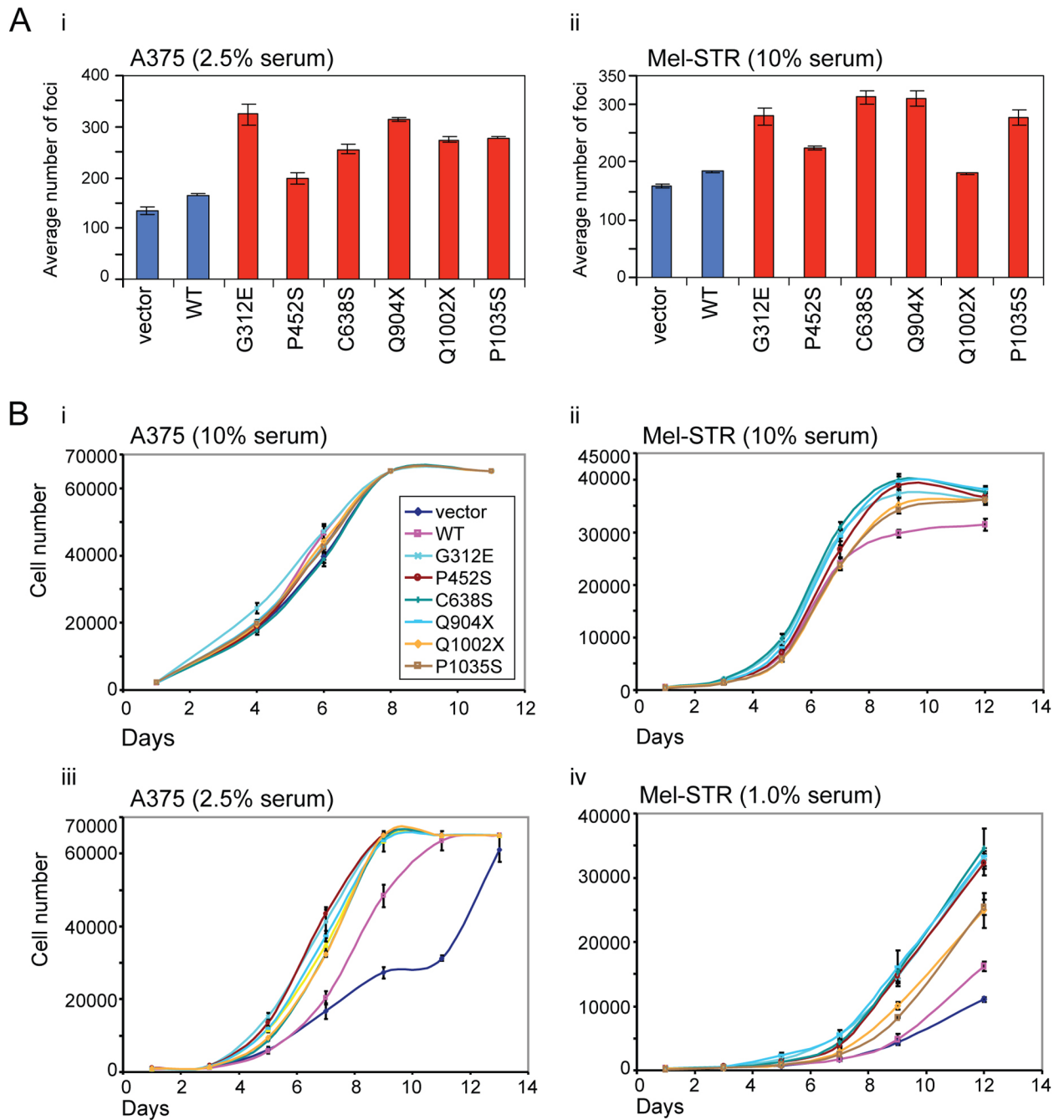


Figure 2. Mutant *ADAMTS18* causes reduced cell dependence on growth factors

(A) Focus formation assay of A375 (i) or Mel-STR (ii) pooled clones expressing the indicated constructs was performed. Graph indicates number of colonies observed after two weeks of growth. (B) Cellular proliferation of A375 (i and iii) or Mel-STR (ii and iv) pooled clones transduced with an empty vector, wild-type *ADAMTS18* or the indicated *ADAMTS18* mutants was assessed in plastic culture plates in the presence of 10% serum (i and ii), or reduced serum (iii and iv) for 12 days. Average cell number at each time point was measured by determining DNA content in eight replicate wells using SYBR Green I.

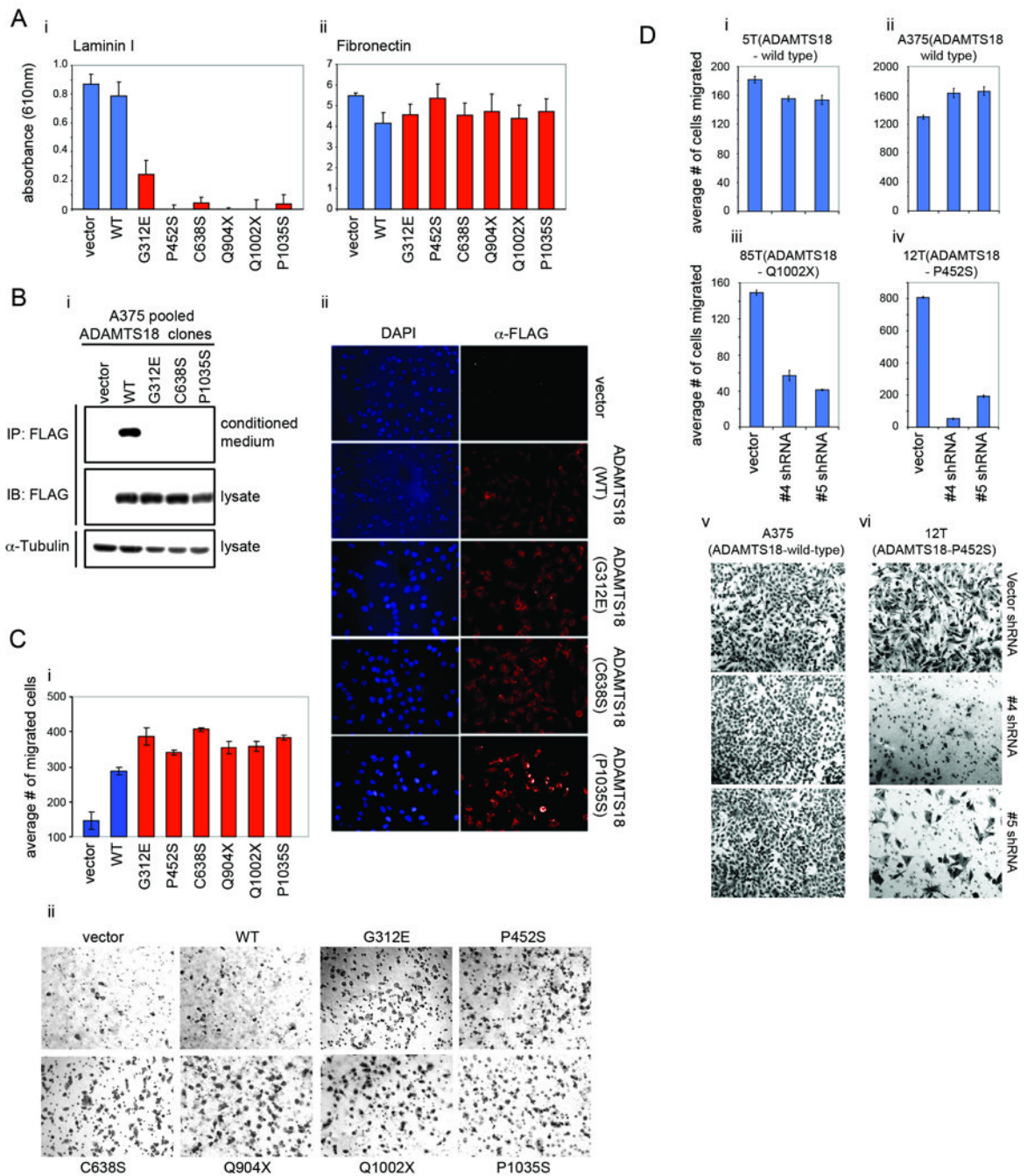


Figure 3. Mutant ADAMTS18 is essential for melanoma cell migration possibly through modulating cell adhesion

(A) Adhesion assay of A375 clones expressing the indicated constructs was performed. Laminin-I (i) or fibronectin (ii) coated plates were assessed for adhesion after 1hr incubation by crystal violet staining. Plates were analyzed by reading the absorbance at 610nm. (B) Localization of ADAMTS18 proteins were assessed using immunoprecipitation and immunofluorescent staining. (i) Cellular condition media and lysates were immunoprecipitated using anti-FLAG (M2) beads and analyzed by western blot analysis. Cell lysates were blotted with anti-alpha-tubulin as a loading control. (ii) A375 pooled ADAMTS-18 clones (WT, G312E, C638S, P1035S or empty vector) were plated and fixed

on slides for immunofluorescent staining with anti-FLAG and DAPI for nuclear localization. (C) A375 clones expressing the indicated constructs were grown in Boyden chambers and assessed for their ability to migrate. (i) Graph indicates the number of cells that migrated 18 hr after seeding (ii) Representative pictures of migrated cells. (D) Melanoma cell lines expressing wild-type ADAMTS18 (i and ii) or mutant ADAMTS18 (iii and iv) were infected with either control shRNAs or two different shRNA constructs targeted against ADAMTS18 (#4 and #5). Migration ability of the cells was assessed and plotted. Representative images of migrated cells are shown in v and vi.

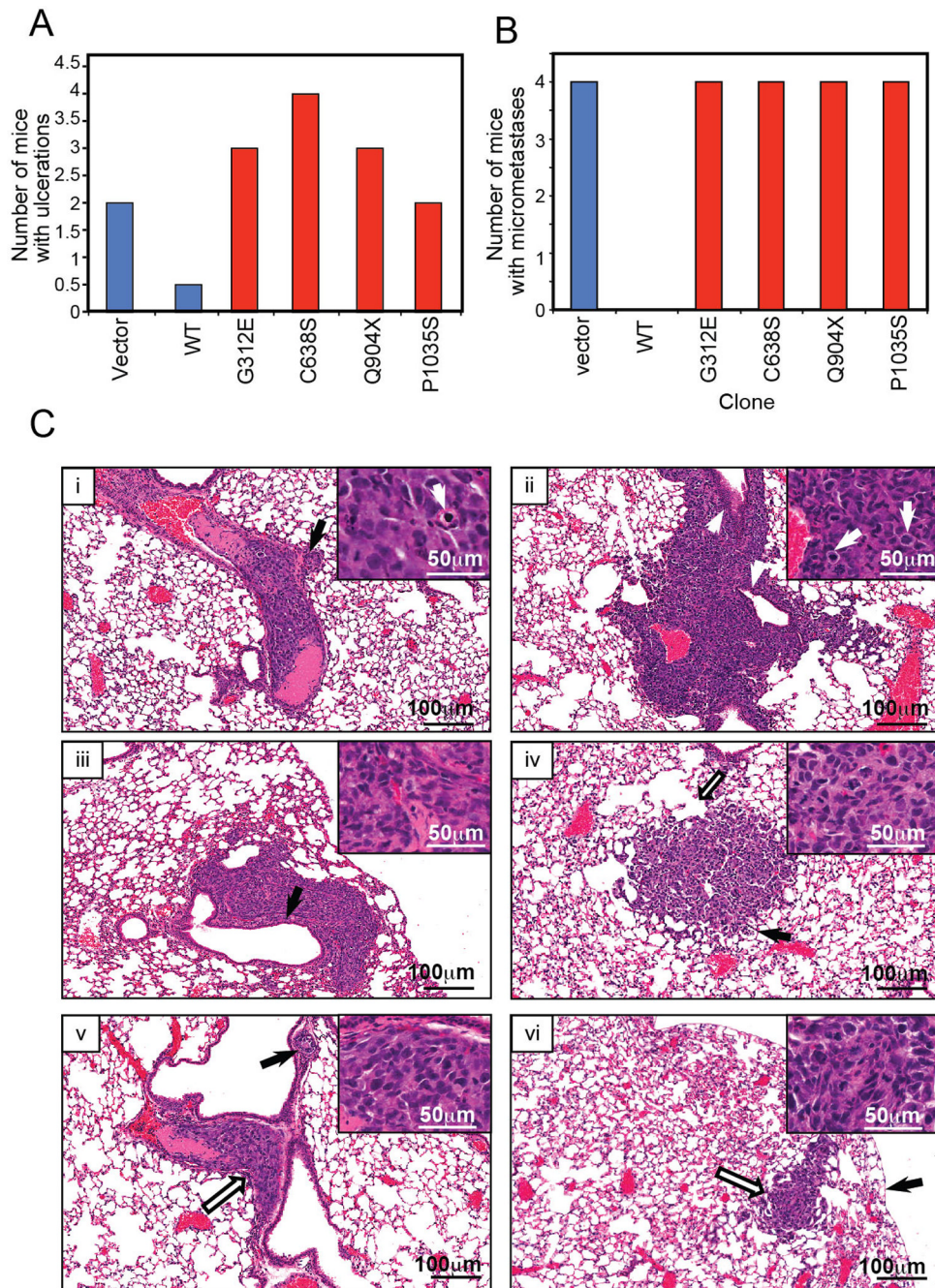


Figure 4. Mutant *ADAMTS18* cause increased lung metastasis in vivo

Mel-STR clones expressing empty vector, wild-type or mutant *ADAMTS18* (G312E, C638S, Q904X, P1035S) were subcutaneously injected into NOD/SCID mice. 22 days after injection, the mice were evaluated for lung metastasis formation by examining hematoxylin/eosin (H&E) stained sections of paraffin embedded lungs. (A) Graph shows the number of mice with ulcerations where 0.5 was used to score minor tumor ulcerations (<2mm) and 1 was used to score major ulcerative tumors (~5–30mm). (B) Graph indicates the number of mice that had lung metastases. (C) Representative images of lung sections showing patterns of metastatic spread of the different mutants and the vector control are presented. (i) Mutant G312E mice, a group of neoplastic cells have impacted into a blood vessel. The malignant

cells are beginning to grow into the lung parenchyma (arrow). The inset at higher magnification shows the characteristic atypia and an apoptotic cell (arrow). (ii) Mutant C638S mice, the metastatic tumor is actively growing and has invaded the surrounding lung tissues. Two bronchi are trapped within the tumor (arrows). Several mitoses are shown in the inset. (iii) Mutant C638S mice, the invading neoplastic tissue grows surrounding a bronchial structure (arrow). The atypia of the malignant cells is evident in the inset. (iv) Mutant Q904X mice, a web-like network of malignant cell is expanding into the lung parenchyma, spilling into alveolar spaces (black arrow). Disruption of the alveolar walls due to altered mechanical properties of the lung tissue is evident in the area surrounding the metastasis (white arrow). (v) Mutant P1035S mice, a group of neoplastic cells have impacted into a blood vessel, and tumor expansions are already growing into the lung (arrow). The cancer cells are shown at a higher magnification in the inset. (vi) Vector mice, a subpleural (black arrow, pleura) metastatic growth (white arrow) is growing into the lung parenchyma. The atypia of the neoplastic cells is shown in the inset.

Table 1

Mutations Identified in ADAMTSS

Gene	Ref Seq accession*	CCDS accession*	No. of mutations (% tumors affected)#	Tumor	Exon	Nucleotide [†]	Amino Acid [‡]	Functional domain
ADAMTSS2	NM_014244.1	CCDS4444.1	5 (5.1%)	71T	3	C655T	P219S	None
				104T	12	G1891A	D631N	None
				104T	18	C2713T	R905C	Thrombospondin type 1 domain
ADAMTSS3	NM_014243	CCDS3553.1	1 (1.3%)	85T	19	C2858T	S953F	Thrombospondin type 1 domain
				55T	22	C3430T	L1144F	None
				32T	22	C3277T	H1093Y	None
ADAMTSS6	NM_197941	CCDS3983.2	3 (2.5%)	85T	3	C629T	S210L	None
				21T	10	G1511A	G504E	None
ADAMTSS7	NM_014272	CCDS32303.1	4 (5.1%)	21T	11	G1513A	E505K	None
				83T	2	C148T	R50X	Propeptide
				63T	2	C377T	P126L	Propeptide
ADAMTSS8	NM_007037	CCDS41732.1	3 (3.8%)	59T	7	G1090A	G364S/LOH	Reprolysin
				4T	16	G2197T	A733S	ADAM-TS Spacer 1
				7T	5	C1289A	A430D	None
ADAMTSS10	NM_030957	CCDS12206.1	4 (3.8%)	16T	6	G1580A	G527E/LOH	ADAM cysteine-rich domain
				48T	7	G1814A	G605E	None
				43T	15	G1936A	E646K	None
ADAMTSS13	NM_139027	CCDS6972.1	2 (2.5%)	55T	21	C2750T	A917V	Thrombospondin type 1 domain
				7T	22	C2791T	P931S/LOH	Thrombospondin type 1 domain
				7T	23	G3193A	G1065S/LOH	None
ADAMTSS15	NM_139055	CCDS8488.1	3 (3.8%)	33T	14	A1652G	D551G	None
				4T	20	C2495T	S832L	None
				24T	3	G1237A	D413N	Reprolysin
ADAMTSS18	NM_199355	CCDS10926.1	14 (17.7%)	32T	8	C2548T	P850S	Thrombospondin type 1 domain
				48T	8	C2642T	A881V	Thrombospondin type 1 domain
				13T	3	G319A	E107K	Propeptide
				44T	5	G851A	R284K	None

Gene	Ref Seq accession*	CCDS accession*	No. of mutations (% tumors affected) [#]	Tumor	Exon	Nucleotide [†]	Amino Acid [‡]	Functional domain
ADAMTS19	NM_133638.3	CCDS4146.1	3 (3.8%)	63T	5	G860A	G287E	None
				23T	5	G935A	G312E	Reprolysin
				12T	9	C1354T	P452S	Reprolysin
				17T	13	T1912A	C638S/LOH	Thrombospondin type 1 domain
				10T	13	G1969A	E657K	None
				36T	14	G2061T	K687N	None
				55T	14	T2081A	F694Y	None
				98T	18	C2710T	Q904X	Thrombospondin type 1 domain
				85T	19	C3004T	Q1002X	Thrombospondin type 1 domain
				104T	20	C3103T	P1035S	Thrombospondin type 1 domain
				71T	21	G3281A	R1094Q	Thrombospondin type 1 domain
				7T	23	C3556T	P1186S	None
				63T	9	G1568A	R523Q	Reprolysin
				16T	14	G2233A	G745R	None
ADAMTS20	NM_025003	CCDS31778.1	12 (11.4%)	91T	19	G2906A	R969Q/LOH	Thrombospondin type 1 domain
				48T	2	C203T	S68F	Propeptide
				32T	4	G684A	M228I	None
				39T	8	C1124T	S375L	Reprolysin
				83T	10	C1442T	S481L	ADAM cysteine-rich domain
				22T	11	G1610A	G537E	ADAM cysteine-rich domain
				74T	13	G1771A	G591R	Thrombospondin type 1 domain
				17T	14	C1957T	R653C	None
				106T	22	C3133T	R1044W	Thrombospondin type 1 domain
				39T	30	G4489A	D1497N	Thrombospondin type 1 domain
55T	36	A5350G	R1784G	GON domain				
55T	38	G5608A	G1870R	GON domain				

* Accession numbers for mutated ADAMTSs in Santa Cruz and GenBank.

Number of non-synonymous mutations observed and percent of tumors affected for each of the 11 genes in the panel of 79 melanoma cancers.

† Nucleotide and amino acid change resulting from mutation.

"X" refers to stop codon. "LOH" refers to cases wherein the wild-type allele was lost and only the mutant allele remained. "None" refers mutations outside any identifiable domain.